Control of Motion and Internal Stresses for a Chain of Two Underactuated Aerial Robots

Marco Tognon[1,2] and Antonio Franchi[1,2]

Abstract— Given the tethered aerial robot problem, in this paper we investigate a multi-agent extension considering a chain of two underactuated flying robots. Our goal is to independently control the elevations (angles) of the two links (or, equivalently, the Cartesian position of the last robot) and their internal stress. For this purpose we theoretically prove the dynamic feedback linearizability of the system and we exploit this property to design a nonlinear controller that exactly linearizes the system. The controller is able to steer the outputs of interest along any trajectory s.t. the desired elevations and stresses are functions of time of class C^3 and C^1, respectively. The controller is able to track independently both positive and negative stresses, i.e., both tension and compression. Resorting to an equivalence argument we then also show the differential flatness of the system. Finally we also demonstrate some of the abilities of the proposed method through numerical examples.

I. INTRODUCTION

In the recent years we saw an increasing popularity of research on *aerial robots*, typically abbreviated as UAVs (Unmanned Aerial Vehicles) or MAVs (Micro Aerial Vehicles). This is due to their extreme versatility that made these robots applicable in a vast range of fields. Nowadays, aerial robots are mainly used as unmanned moving sensors for information gathering applications such as surveillance, shared control, agriculture and civil monitoring, search and rescue and so on [1], [2]. Nevertheless, the physical interaction problem is becoming the center of several researches in aerial robotics, see, e.g., [3] and references therein. For example many works are done in order to exploit aerial robots for manipulation and transportation of loads [4], [5].

An interesting related problem is the control of a tethered aerial vehicle to a fixed or moving ground station. The use of a link between the robot and the ground, introduces many advantages: first of all, for application such as surveillance, monitoring and temporary communication network relays, the cable can be exploited to provide energy and a constant high-bandwidth communication channel to the robot [6], [7]. Furthemore, it was shown that the tethered flight system can be a solution to improve the hover stability during dangerous maneuvers or in the presence of disturbances, e.g., during operations of landing and take off from non static platform as a ship during rough sea (see, e.g., [8] and references therein).

In [9] it is presented a controller able to stabilize the elevation of the tethered aerial robot to a constant value,

[1]CNRS, LAAS, 7 Avenue du Colonel Roche, F-31400 Toulouse, France. `mtognon@laas.fr`, `antonio.franchi@laas.fr`
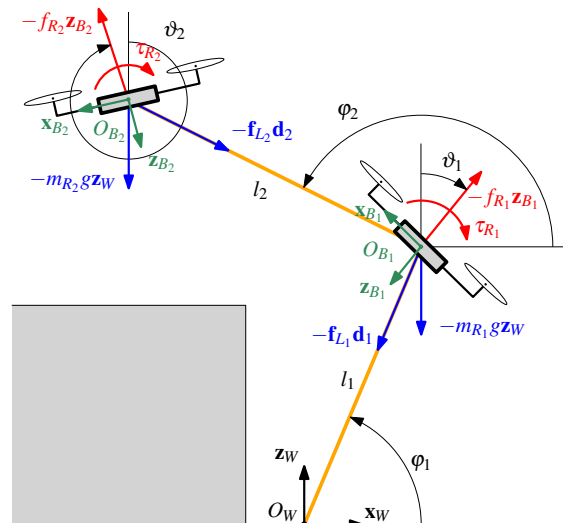[2]Univ de Toulouse, LAAS, F-31400 Toulouse, France

Fig. 1: Representation of the system and its main variables. The system is depicted in a scenario of example where the grey box represents a surface of manipulation for, e.g., a pick and place task.

closing the control feedback with an estimator that recovers the state using only inertial onboard sensors. Real experiments based on a tethered quadrotor are presented as well. Some recently proposed controller takes into account not only the link elevation but also its tension. In fact, in [10] is presented a method able to stabilize the elevation while ensuring always positive tension. Finally, an advanced control/observer method, shown in [11], is able to track any time-varying desired trajectory of both the elevation and the stress (tension or compression) of a generic link, resorting only to standard onboard inertial sensors.

In this paper we solve a more complex case with respect to the single tethered aerial vehicle problem considered in [9]–[11]. The studied system consists of two aerial robots connected to each other and to the ground by two links, i.e., a chain of two robots attached to a fixed point by two links. The considered system can be seen as the combination of a planar two-link robot with two flying aerial systems. In fact, similarly to a two-link robot, this system can reach any point on the vertical plane, thus achieving a tremendous increase of the workspace with respect to the one of the single tethered aerial robot considered in the literature so far.

The two control objectives solved in this work are recapped in the following. First of all, we aim at tracking any time-varying desired configuration for the two links. In other words, by the inverse kinematic, we aim at tracking any Cartesian trajectory of the end of the chain, comparable

to the end-effector of a planar two-link robot. Secondly, we consider the tracking problem of any time-varying trajectory of the stress applied to the links. In order to be as general as possible we consider generic links that permits only tension in the case of cables, or both tension and compression in the case of beams.

For these purposes, we present in this paper a novel controller based on the dynamic feedback linearization technique able to achieve the independent tracking of the two variables of interest. The controller allows to, e.g., execute pick and place operations with the second robot, while a precise stress can be controlled, ensuring positive tension in the case of cable, and avoiding breakages due to excessive stresses.

The paper is organized as follows. In Sec. II we derive the dynamic model of the system, writing an explicit characterization of the stress on the two links. In the following Sec. III we design the controller for the elevation and stress of the links based on the feedback linearization method. The verification of the proposed controller is presented in Sec. IV by simulations. Conclusions and future developments are shown in Sec. V.

II. DYNAMIC MODEL

We consider a multi agent extension of the original problem defined in [9]–[11] by looking at a system composed by two underactuated flying vehicles lying on a vertical plane that are connected to the ground and to each others through two *links*, as depicted in Fig. 1. One can see the similarity with a two-link Cartesian robot where the end of the chain represents the end-effector, while the aerial vehicles are the actuated joints of the robot.

In order to refer to the quantities of one component of the chain, we use the subscript $\cdot_i$ with $i = 1$ for the first link and $i = 2$ for the second. Similarly to [9]–[11] we assume: (i) link masses and rotational inertias are negligible with respect to the ones of the vehicles, (ii) fixed link lengths $l_i \in \mathbb{R}_{>0}$ where $i \in \{1, 2\}$, and (iii) negligible deformations and elasticities.

We define $\varphi_i \in \mathbb{R}$ the angle that the i-th link forms with the horizon, called *elevation*. With $f_{Li} \in \mathbb{R}$ we denote the internal force that is exerted on the i-th link along its longitudinal line, called *link stress*. The stress is called *tension* if the link is pulled, i.e., $f_L > 0$, viceversa, it is called *compression* if the link is compressed, i.e., $f_L < 0$.

With respect to [9]–[11], here we consider three more 'challenges'. First of all we extend the problem to a multi agent system composed by two link-vehicle components. Then, of this system, we aim to control not only the elevation but also the stress of the two links. Moreover we want to obtain the tracking of the output of interest along any desired time-varying trajectory, instead of just achieving regulation to constant values.

The first link is connected at one end to the center of mass (CoM) of the first vehicle, and the other end to a *fixed point*. The two ends of the second link are attached to the first and second vehicle center of masses, respectively. No rotational constraints are present in the connections, e.g., by using passive rotational joints. Finally, each aerial vehicle is modeled as a rigid body characterized by mass $m_{Ri} \in \mathbb{R}_{>0}$ and rotational inertia $J_{Ri} \in \mathbb{R}_{>0}$, with $i = 1, 2$.

It is convenient to define the frames of the system in 3D, even if we consider a 2D problem, in order, e.g., to have a well defined angular velocity vector for the aerial vehicles. Thus we define a *world frame*, $\mathscr{F}_W$, described by the unit vector along its axes $\{\mathbf{x}_W, \mathbf{y}_W, \mathbf{z}_W\}$ and origin set on a fixed point O_W. Then, for every robot, we define a *body frame*, $\mathscr{F}_{Bi}$, rigidly attached to the i-th vehicle, described by the unit vector along its axes $\{\mathbf{x}_{Bi}, \mathbf{y}_{Bi}, \mathbf{z}_{Bi}\}$ and origin O_{Bi} set on the vehicle CoM, represented in $\mathscr{F}_W$ by the coordinates $\mathbf{p}_{Bi} = [x_{Bi} \ y_{Bi} \ z_{Bi}]^T$, where $y_{Bi} = 0$. The axes $\mathbf{y}_W$, $\mathbf{y}_{B_1}$ and $\mathbf{y}_{B_2}$ are perpendicular to the vertical plane $\{\mathbf{x}_W, \mathbf{z}_W\}$ where motion occurs, as depicted in Fig. 1. The system evolves on this vertical plane on the effect of the four control inputs (two for each robot), i.e., the intensities $f_{Ri} \in \mathbb{R}$ and $\tau_{Ri} \in \mathbb{R}$ of the thrust force $-f_{Ri}\mathbf{z}_{Bi} \in \mathbb{R}^3$ and the torque $-\tau_{Ri}\mathbf{y}_{Bi} \in \mathbb{R}^3$, respectively, with $i = 1, 2$[1].

Given the constraints, the system is completely described by the generalized coordinates $\mathbf{q} = (\varphi_1, \varphi_2, \vartheta_1, \vartheta_2)$, where φ_i and ϑ_i are the *elevation* of the i-th link (defined before) and the *attitude* of the i-th vehicle, respectively.

Kinetic and potential energy of the system are given, respectively, by:

$$K = \frac{1}{2}\dot{\boldsymbol{\varphi}}^T \mathbf{M}(\boldsymbol{\varphi})\dot{\boldsymbol{\varphi}} + \frac{1}{2}\dot{\boldsymbol{\vartheta}}^T \mathbf{J}_R \dot{\boldsymbol{\vartheta}}$$
$$V = g[(m_{R1} + m_{R2})l_1 \sin\varphi_1 + m_{R2}l_2 \sin\varphi_2],$$

where g is the gravitational constant, $\boldsymbol{\varphi} = [\varphi_1 \ \varphi_2]^T$, $\boldsymbol{\vartheta} = [\vartheta_1 \ \vartheta_2]^T$ and

$$\mathbf{M}(\boldsymbol{\varphi}) = \begin{bmatrix} (m_{R1} + m_{R2})l_1^2 & m_{R2}l_1l_2 \cos(\varphi_1 - \varphi_2) \\ m_{R2}l_1l_2 \cos(\varphi_1 - \varphi_2) & m_{R2}l_2^2 \end{bmatrix}$$

$$\mathbf{J}_R = \begin{bmatrix} J_{R1} & 0 \\ 0 & J_{R2} \end{bmatrix}.$$

The generalized forces $\mathbf{Q_q} = (\mathbf{Q}_{\boldsymbol{\varphi}}, \mathbf{Q}_{\boldsymbol{\vartheta}})$ of the system are

$$\mathbf{Q}_{\boldsymbol{\varphi}} = \underbrace{\begin{bmatrix} l_1 \cos(\varphi_1 + \vartheta_1) & l_1 \cos(\varphi_1 + \vartheta_2) \\ 0 & l_2 \cos(\varphi_2 + \vartheta_2) \end{bmatrix}}_{\bar{\mathbf{Q}}_{\boldsymbol{\varphi}}(\boldsymbol{\varphi}, \boldsymbol{\vartheta})} \begin{bmatrix} f_{R1} \\ f_{R2} \end{bmatrix}$$

$$\mathbf{Q}_{\boldsymbol{\vartheta}} = \begin{bmatrix} \tau_{R1} \\ \tau_{R2} \end{bmatrix}.$$

Then, applying the Euler-Lagrange equation, we obtain

$$\mathbf{M}(\boldsymbol{\varphi})\ddot{\boldsymbol{\varphi}} = -\mathbf{c}(\boldsymbol{\varphi}, \dot{\boldsymbol{\varphi}}) + \bar{\mathbf{Q}}_{\boldsymbol{\varphi}}(\boldsymbol{\varphi}, \boldsymbol{\vartheta})\mathbf{f}_R \quad (1)$$
$$\mathbf{J}_R \ddot{\boldsymbol{\vartheta}} = \boldsymbol{\tau}_R, \quad (2)$$

where $\mathbf{f}_R = [f_{R1} \ f_{R2}]^T$, $\boldsymbol{\tau}_R = [\tau_{R1} \ \tau_{R2}]^T$, and

$$\mathbf{c}(\boldsymbol{\varphi}, \dot{\boldsymbol{\varphi}}) = \begin{bmatrix} m_{R2}l_1l_2 \sin(\varphi_1 - \varphi_2)\dot{\varphi}_2^2 + (m_{R1} + m_{R2})gl_1 \cos\varphi_1 \\ -m_{R2}l_1l_2 \sin(\varphi_1 - \varphi_2)\dot{\varphi}_1^2 + m_{R2}gl_2 \cos\varphi_2 \end{bmatrix}$$

contains the centrifugal and gravitational terms.

We shall now write down the expression of the stresses f_{L1} and f_{L2}. Since we are considering the 2D problem, in

---

[1]For generality we consider both positive and negative thrust. Although generally aerial vehicles can provide only positive thrust, actually, the variable pitch solution can provide negative thrust as well [12]. However, if only positive thrust is allowed, our controller is still valid, since this constraint can be meet in the planning phase as explained later in the paper.

the following, we will omit the lines full of zeros relative to the $\mathbf{y}_{B_1}$ and $\mathbf{y}_{B_2}$ axes. Balancing the forces acting on the vehicle CoMs we obtain

$$\underbrace{\begin{bmatrix} m_1\ddot{\mathbf{p}}_{B_1} \\ m_2\ddot{\mathbf{p}}_{B_2} \end{bmatrix}}_{\mathbf{a}} = -\underbrace{\begin{bmatrix} \mathbf{d}_1 f_{L1} - \mathbf{d}_2 f_{L2} \\ \mathbf{d}_2 f_{L2} \end{bmatrix}}_{\mathbf{a}_{f_L}} - \underbrace{\begin{bmatrix} f_{R1}\mathbf{z}_{B_1} \\ f_{R2}\mathbf{z}_{B_2} \end{bmatrix}}_{\mathbf{a}_{f_R}} - \underbrace{\begin{bmatrix} m_{R1}g\mathbf{z}_W \\ m_{R2}g\mathbf{z}_W \end{bmatrix}}_{\mathbf{a_g}}, \quad (3)$$

where $\mathbf{d}_i = [\cos\varphi_i \; \sin\varphi_i]^T$ and $\mathbf{d}_i^\perp = [-\sin\varphi_i \; \cos\varphi_i]^T$ are unit vectors in the vertical plane parallel and perpendicular to the i-th link, respectively. The accelerations of the vehicle CoMs expressed in $\mathscr{F}_W$ are

$$\begin{aligned} \ddot{\mathbf{p}}_{B_1} &= -l_1\mathbf{d}_1\dot{\varphi}_1^2 + l_1\mathbf{d}_1^\perp\ddot{\varphi}_1 \\ \ddot{\mathbf{p}}_{B_2} &= \ddot{\mathbf{p}}_{B_1} - l_2\mathbf{d}_2\dot{\varphi}_2^2 + l_2\mathbf{d}_2^\perp\ddot{\varphi}_2. \end{aligned} \quad (4)$$

Using (4) and (3) we have that

$$\mathbf{a} = \underbrace{\begin{bmatrix} -m_{R1}l_1\mathbf{d}_1\dot{\varphi}_1^2 \\ -m_{R2}(l_1\mathbf{d}_1\dot{\varphi}_1^2 + l_1\mathbf{d}_2\dot{\varphi}_2^2) \end{bmatrix}}_{\mathbf{a}_{\boldsymbol{\varphi}}} + \underbrace{\begin{bmatrix} m_{R1}l_1\mathbf{d}_1^\perp & \mathbf{0} \\ m_{R2}l_1\mathbf{d}_1^\perp & m_{R2}l_2\mathbf{d}_2^\perp \end{bmatrix}}_{\mathbf{A}_{\ddot{\boldsymbol{\varphi}}}}\ddot{\boldsymbol{\varphi}}$$

$$\mathbf{a}_{\mathbf{f}_L} = \underbrace{\begin{bmatrix} \mathbf{d}_1 & -\mathbf{d}_2 \\ \mathbf{0} & \mathbf{d}_2 \end{bmatrix}}_{\mathbf{D}}\mathbf{f}_L,$$

where $\mathbf{a}_{\boldsymbol{\varphi}} \in \mathbb{R}^4$, $\mathbf{A}_{\ddot{\boldsymbol{\varphi}}} \in \mathbb{R}^{4\times 2}$, $\mathbf{D} \in \mathbb{R}^{4\times 2}$ and $\mathbf{f}_L = [f_{L1} \; f_{L2}]^T$. Therefore (3) can be rewritten as:

$$\underbrace{\begin{bmatrix} \mathbf{A}_{\ddot{\boldsymbol{\varphi}}} & \mathbf{D} \end{bmatrix}}_{\mathbf{W}}\begin{bmatrix} \ddot{\boldsymbol{\varphi}} \\ \mathbf{f}_L \end{bmatrix} = -\mathbf{a}_{\mathbf{f}_R} - \mathbf{a_g} - \mathbf{a}_{\boldsymbol{\varphi}}. \quad (5)$$

The matrix $\mathbf{W} \in \mathbb{R}^{4\times 4}$, that can be explicitly written as

$$\mathbf{W} = \begin{bmatrix} -l_1 m_{R1}\sin\varphi_1 & 0 & \cos\varphi_1 & -\cos\varphi_2 \\ l_1 m_{R1}\cos\varphi_1 & 0 & \sin\varphi_1 & -\sin\varphi_2 \\ -l_1 m_{R2}\sin\varphi_1 & -l_2 m_{R2}\sin\varphi_2 & 0 & \cos\varphi_2 \\ l_1 m_{R2}\cos\varphi_1 & l_2 m_{R2}\cos\varphi_2 & 0 & \sin\varphi_2 \end{bmatrix},$$

is full rank, in fact its determinant is

$$\det(\mathbf{W}) = -l_1 l_2 m_{R2}[m_{R1} + m_{R2}(1 - \cos^2(\varphi_1 - \varphi_2))],$$

which is always nonzero.

Thus, in order to find the expression of the stresses $\mathbf{f}_L$ we can invert (5) and select only the last two components

$$\mathbf{f}_L = \underbrace{\begin{bmatrix} \mathbf{0} & \mathbf{I}_2 \end{bmatrix}\mathbf{W}^{-1}}_{\mathbf{W}_{\mathbf{f}_L} \in \mathbb{R}^{2\times 4}}(-\mathbf{a}_{\mathbf{f}_R} - \mathbf{a_g} - \mathbf{a}_{\boldsymbol{\varphi}}).$$

In this paper we aim at designing a control law for the inputs (f_{R1}, τ_{R1}) and (f_{R2}, τ_{R2}) that is able to asymptotically steer $(\boldsymbol{\varphi}, \mathbf{f}_L)$ along any smooth desired trajectory $(\boldsymbol{\varphi}^d, \mathbf{f}_L^d)$.

Remark 1 (Differences Between Bar and Cable). The considered control problem is mainly focused on systems where the aerial vehicles are tethered by cables, as progression of previous works [9]–[11]. In this contest the assumption of negligible mass and inertia of the link is valid for the majority of practical problems. Though, using cable, only tension are suitable. While, for a bar, to allow also compression without deformations, it must have mechanical characteristics that could invalidate the assumption of negligible mass and inertia. In this work we consider both cables and bars with

negligible mass and inertia in order to be more general and to proof the validity of our approach providing both tension an compression. The extension considering mass and inertial of the links in the model will be investigated in future works.

III. CONTROLLER

In order to design a control law that fulfills our control objectives, we first rewrite the system in state space form by defining $\mathbf{x} = \begin{bmatrix} \varphi_1 & \varphi_2 & \vartheta_1 & \vartheta_2 & \dot{\varphi}_1 & \dot{\varphi}_2 & \dot{\vartheta}_1 & \dot{\vartheta}_2 \end{bmatrix}^T = \begin{bmatrix} \boldsymbol{\varphi}^T & \boldsymbol{\vartheta}^T & \dot{\boldsymbol{\varphi}}^T & \dot{\boldsymbol{\vartheta}}^T \end{bmatrix}^T = \begin{bmatrix} \mathbf{x}_1^T & \mathbf{x}_2^T & \mathbf{x}_3^T & \mathbf{x}_4^T \end{bmatrix}^T \in \mathbb{R}^8$ and $\mathbf{u} = \begin{bmatrix} f_{R1} & f_{R2} & \tau_{R1} & \tau_{R2} \end{bmatrix}^T = \begin{bmatrix} \mathbf{f}_R^T & \boldsymbol{\tau}_R^T \end{bmatrix}^T = \begin{bmatrix} \mathbf{u}_1^T & \mathbf{u}_2^T \end{bmatrix}^T \in \mathbb{R}^4$ as the state and input vectors of the system, respectively. We can then rewrite (1) and (2) in the state-space form as

$$\dot{\mathbf{x}}_1 = \mathbf{x}_3 \quad (6a)$$
$$\dot{\mathbf{x}}_2 = \mathbf{x}_4 \quad (6b)$$
$$\dot{\mathbf{x}}_3 = -\mathbf{M}^{-1}\mathbf{c} + \mathbf{M}^{-1}\bar{\mathbf{Q}}_{\boldsymbol{\varphi}}\mathbf{u}_1 \quad (6c)$$
$$\dot{\mathbf{x}}_4 = \mathbf{J}_R^{-1}\mathbf{u}_2 \quad (6d)$$

where the inversion of $\mathbf{M}$ is always possible being

$$\det(\mathbf{M}) = l_1^2 l_2^2 m_{R2}[m_{R1} + m_{R2}(1 - \cos^2(\varphi_1 - \varphi_2))]$$

always nonzero.

To control the elevations and the stresses of the two links, we consider as outputs of the system the variables $\mathbf{y} = \begin{bmatrix} \varphi_1 & \varphi_2 & f_{L1} & f_{L2} \end{bmatrix}^T = \begin{bmatrix} \boldsymbol{\varphi}^T & \mathbf{f}_L^T \end{bmatrix}^T = \begin{bmatrix} \mathbf{y}_1^T & \mathbf{y}_2^T \end{bmatrix}^T \in \mathbb{R}^4$. In the following proposition, which represents the main result of this paper, we show that it is possible to completely transform the non linear system in an equivalent controllable and decoupled linear system.

Proposition 1. *Consider the system composed by two aerial vehicles connected in series to the ground by two links with passive joints, whose dynamic model is described by (6). Consider as outputs the elevation and the stress of the two links, $\mathbf{y} = [\boldsymbol{\varphi}^T \; \mathbf{f}_L^T]^T$. Then the system is fully linearizable via dynamic feedback for every state configuration, iff both thrusts f_{R1} and f_{R2} are nonzero.*

Proof. First of all, we need to differentiate the outputs until the inputs appear. Inverting (5), recalling that $\mathbf{y}_1^{(2)} = \ddot{\boldsymbol{\varphi}}$ and $\mathbf{y}_2 = \mathbf{f}_L$, we directly obtain

$$\begin{bmatrix} \mathbf{y}_1^{(2)} \\ \mathbf{y}_2 \end{bmatrix} = \mathbf{W}^{-1}(-\mathbf{a_g} - \mathbf{a}_{\boldsymbol{\varphi}}) + \underbrace{\left(-\mathbf{W}^{-1}\begin{bmatrix} \mathbf{Z}_R & \mathbf{0} \end{bmatrix}\right)}_{\mathbf{E}(\mathbf{x})}\mathbf{u}, \quad (7)$$

where $\bullet^{(n)} = \frac{d^n \bullet}{dt^n}$ indicates the n-th time-derivative, for $n \geq 1$, and $\mathbf{Z}_R \in \mathbb{R}^{4\times 2}$ is defined by

$$\mathbf{a}_{\mathbf{f}_R} = \begin{bmatrix} \mathbf{z}_{B_1} & \mathbf{0} & \mathbf{0} & \mathbf{0} \\ \mathbf{0} & \mathbf{z}_{B_2} & \mathbf{0} & \mathbf{0} \end{bmatrix}\mathbf{u} = \begin{bmatrix} \mathbf{Z}_R & \mathbf{0} \end{bmatrix}\mathbf{u}.$$

From (7) we can see that the input appears directly in $\mathbf{y}_2$ without need for differentiation while $\mathbf{y}_1$ has to be differentiated twice. Furthermore, we can immediately notice that the decoupling matrix $\mathbf{E}(\mathbf{x})$ is always singular which means that it is not possible to determine a static feedback that linearizes the system using $\mathbf{y}$.

In these cases, the common technique is to delay the appearance of the input in $\mathbf{y}_2$ (i.e., increasing the relative degree of $\mathbf{y}_2$) introducing a dynamic compensator composed by one or more integrators in the input channel $\mathbf{u}_1$.

To this aim, we redefine the input as $\bar{\mathbf{u}} = \begin{bmatrix} \ddot{\mathbf{u}}_1^T & \mathbf{u}_2^T \end{bmatrix}^T = \begin{bmatrix} \bar{\mathbf{u}}_1^T & \bar{\mathbf{u}}_2^T \end{bmatrix}^T$, considering the acceleration of the thrust intensity as new controllable input, $\ddot{\mathbf{u}}_1 = \ddot{\mathbf{f}}_R$. The system is now described by the extended state $\bar{\mathbf{x}} = \begin{bmatrix} \boldsymbol{\varphi}^T & \dot{\boldsymbol{\varphi}}^T & \boldsymbol{\vartheta}^T & \dot{\boldsymbol{\vartheta}}^T & \mathbf{u}_1^T & \dot{\mathbf{u}}_1^T \end{bmatrix}^T \in \mathbb{R}^{12}$, that contains also the thrusts and their derivatives. Considering the extended system and the new input, $\mathbf{y}_1$ and $\mathbf{y}_2$ have to be differentiated four and two times, respectively, in order to see the new input $\bar{\mathbf{u}}$ appear:

$$\begin{bmatrix} \mathbf{y}_1^{(4)} \\ \mathbf{y}_2^{(2)} \end{bmatrix} = (\mathbf{W}^{-1})(-\ddot{\mathbf{a}}_{\mathbf{f}_R} - \mathbf{a}_\mathbf{g} - \mathbf{a}_{\boldsymbol{\varphi}}) + 2(\dot{\mathbf{W}^{-1}})(-\dot{\mathbf{a}}_{\mathbf{f}_R} - \dot{\mathbf{a}}_{\boldsymbol{\varphi}}) + \qquad (8)$$
$$+ (\ddot{\mathbf{W}^{-1}})(-\ddot{\mathbf{a}}_{\mathbf{f}_R} - \ddot{\mathbf{a}}_{\boldsymbol{\varphi}}).$$

In the previous equation the inputs appear only in the term $\ddot{\mathbf{a}}_{\mathbf{f}_R}$ that can be rewritten as:

$$\ddot{\mathbf{a}}_{\mathbf{f}_R} = \ddot{\mathbf{a}}'_{\mathbf{f}_R}(\bar{\mathbf{x}}) + \ddot{\mathbf{A}}''_{\mathbf{f}_R}(\bar{\mathbf{x}})\bar{\mathbf{u}},$$

where

$$\ddot{\mathbf{A}}''_{\mathbf{f}_R}(\bar{\mathbf{x}}) = \begin{bmatrix} -\sin\vartheta_1 & 0 & -\frac{f_{R1}\cos\vartheta_1}{J_{R1}} & 0 \\ -\cos\vartheta_1 & 0 & \frac{f_{R1}\sin\vartheta_1}{J_{R1}} & 0 \\ 0 & -\sin\vartheta_2 & 0 & -\frac{f_{R2}\cos\vartheta_2}{J_{R2}} \\ 0 & -\cos\vartheta_2 & 0 & \frac{f_{R2}\sin\vartheta_2}{J_{R2}} \end{bmatrix}.$$

We can compactly rewrite (8) as:

$$\begin{bmatrix} \mathbf{y}_1^{(4)} \\ \mathbf{y}_2^{(2)} \end{bmatrix} = \mathbf{b}(\bar{\mathbf{x}}) + \underbrace{\left(-\mathbf{W}^{-1}\ddot{\mathbf{A}}''_{\mathbf{f}_R}(\bar{\mathbf{x}}) \right)}_{\bar{\mathbf{E}}(\bar{\mathbf{x}})} \bar{\mathbf{u}}, \qquad (9)$$

where $\mathbf{b}(\bar{\mathbf{x}})$, whose expression is omitted here for the sake of brevity, collects all the terms in (8) that do not depend on the input. After some algebra, it is possible to analytically compute the determinant of the new decoupling matrix $\bar{\mathbf{E}}(\bar{\mathbf{x}})$:

$$\det\left(\bar{\mathbf{E}}(\bar{\mathbf{x}})\right) = -\frac{f_{R1}f_{R2}}{J_{R1}J_{R2}l_1l_2m_{R2}\left(m_{R1} + m_{R2}\sin^2(\varphi_1 - \varphi_2)\right)},$$

which is zero iff $f_{R1} = 0$ or $f_{R2} = 0$. Therefore $\bar{\mathbf{E}}(\bar{\mathbf{x}})$ is always invertible except for the zero measure cases in which one of the two thrusts vanishes.

Furthermore the total relative degree[2] $r = 8 + 4 = 12$ is equal to the dimension of the extended state $\bar{\mathbf{x}}$. This means that the system does not have an internal dynamics [13], i.e., it is fully linearizable through dynamic feedback.

In fact, designing the control input as

$$\bar{\mathbf{u}} = \bar{\mathbf{E}}^{-1}(\bar{\mathbf{x}})\left[-\mathbf{b}(\bar{\mathbf{x}}) + \mathbf{v}\right], \qquad (10)$$

where $\mathbf{v} = [\mathbf{v}_1^T \ \mathbf{v}_2^T]^T \in \mathbb{R}^4$ is a virtual input, we obtain

$$\mathbf{y}_1^{(4)} = \mathbf{v}_1 \qquad \mathbf{y}_2^{(2)} = \mathbf{v}_2,$$

[2]i.e., the sum, for each element of the output, of the number of times that each output entry has to be differentiated in order to see the input appear.
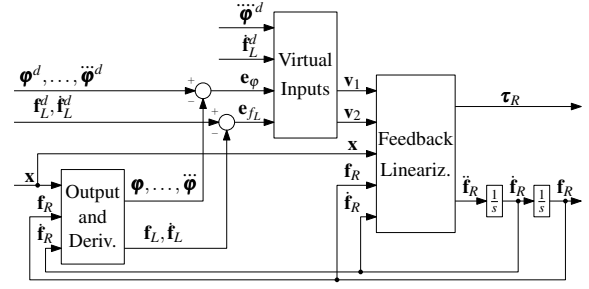

Fig. 2: Graphic representation of the controller.

i.e., through the state feedback transformation (10) we transform the original non linear system (6) in a fully-equivalent linear and decoupled dynamical system. □

The next result is a consequence of the previous Proposition 1 and presents the overall controller design, which is also depicted in Fig. 2.

Corollary 1. *Let be given any desired trajectory $\mathbf{y}_1^d(t)$ of class C^3 for the two links elevation $\mathbf{y}_1$, and any desired trajectory $\mathbf{y}_2^d(t)$ of class C^1 for the two links stress $\mathbf{y}_2$. Consider as input the second derivative of the two thrusts and the torques provided by the aerial vehicles, $\bar{\mathbf{u}} = [\ddot{\mathbf{f}}_R^T \ \boldsymbol{\tau}_R^T]^T$. Consider the control law described by (10) and set the virtual inputs as:*

$$\mathbf{v}_1 = \mathbf{y}_1^{d(4)} + \mathbf{K}_{11}\mathbf{e}_1 + \mathbf{K}_{12}\mathbf{e}_1^{(1)} + \mathbf{K}_{13}\mathbf{e}_1^{(2)} + \mathbf{K}_{14}\mathbf{e}_1^{(3)}$$
$$\mathbf{v}_2 = \mathbf{y}_2^{d(2)} + \mathbf{K}_{21}\mathbf{e}_2 + \mathbf{K}_{22}\mathbf{e}_2^{(1)}, \qquad (11)$$

where $\mathbf{K}_{ij} \in \mathbb{R}_{>0}^{2\times2}$, with $i = 1\ldots4$ and $j = 1,2$, are diagonal matrices.

That control law exponentially steers $\mathbf{y}$ along any desired trajectory $\mathbf{y}^d = [\varphi_1^d \ \varphi_2^d \ f_{L1}^d \ f_{L2}^d]^T$. The behavior of the convergence can be arbitrarily assigned by suitably choosing the gain matrixes.

Proof. Let us define the errors as $\mathbf{e}_1 = \mathbf{y}_1^d - \mathbf{y}_1$ and $\mathbf{e}_2 = \mathbf{y}_2^d - \mathbf{y}_2$. The controller yields to the following error dynamics:

$$\mathbf{e}_1^{(4)} + \mathbf{K}_{11}\mathbf{e}_1 + \mathbf{K}_{12}\mathbf{e}_1^{(1)} + \mathbf{K}_{13}\mathbf{e}_1^{(2)} + \mathbf{K}_{14}\mathbf{e}_1^{(3)} = 0$$
$$\mathbf{e}_2^{(2)} + \mathbf{K}_{21}\mathbf{e}_2 + \mathbf{K}_{22}\mathbf{e}_2^{(1)} = 0.$$

Therefore, from basic linear system theory, one can arbitrarily assign the poles of the dynamics of the error in order to guaranties an arbitrarily fast exponential tracking of $(\mathbf{y}_1^d(t), \mathbf{y}_2^d(t))$ for $(\mathbf{y}_1(t), \mathbf{y}_2(t))$ by suitably choosing the gains: $\bar{\mathbf{K}}_1 = [\mathbf{K}_{11} \ \mathbf{K}_{12} \ \mathbf{K}_{13} \ \mathbf{K}_{14}] \in \mathbb{R}_{>0}^{2\times8}$ and $\bar{\mathbf{K}}_2 = [\mathbf{K}_{21} \ \mathbf{K}_{22}] \in \mathbb{R}_{>0}^{2\times4}$. Since $(\mathbf{y}_1^{d(4)}(t), \mathbf{y}_2^{d(2)}(t))$ have to be well defined, the elevation and stress trajectories have to be of class C^3 and C^1 respectively. □

Due to Proposition 1, if the links are bars, it is feasible to pass from compression to tension and viceversa. Instead, in the case of a cable, it is possible to maintain a sufficient value of tension under a maximum breaking value an above the minimum tautness value.

We remark that, since the total relative degree is equal to the dimension of the extended state, there is no internal

dynamics. This implies that the dynamics of the pitch of each vehicles is stable during the tracking of the desired output.

Remark 2 (Initial Cable Pre-Tension). In the case that the link is a tie (like a cable) a preliminary phase has to bring the link in a taut condition, in order to make the model valid. As shown in [3], using a near hovering controller, following a radial trajectory away from the fixed point, we are able to reach the initial position and to provide a sufficient force to make the tie taut. Then the control can be switched on and used to control the stress in the positive domain. In fact, when the tie is taut it can be approximated as a rigid body and the non-deformability assumption is also well defined.

Remark 3 (Case of zero thrust). If a particular desired trajectory of the outputs requires zero thrust on one of the two vehicles the controller cannot be applied, indeed in this case it has a singularity. Thus, this fact has to be considered in the planning phase in order to design desired trajectories that ensure strictly positive, or negative, thrusts. Although this is a planning problem that does not concern this work, we believe that the problem of zero thrust does not imply a strong limitation on the set of the feasible trajectories. Indeed, as it is shown in Sec. IV, we can still generate non-trivial trajectories, e.g., inversion of the stress from tension to compression, ensuring non zero thrusts. An extended study on the planning of feasible trajectories is left as future work.

Looking at the control law described by the equations (10) and (11), and depicted in the block diagram of Fig. 2, one can notice that its implementation requires the knowledge of the extended state $\bar{\mathbf{x}}$, the output $\mathbf{y}$ and its derivatives (up to the third-order for $\mathbf{y}_1$ and first-order for $\mathbf{y}_2$). Nevertheless, $\mathbf{y}$ and all its needed derivatives can be calculated as function of $\mathbf{x}$ and $\bar{\mathbf{u}}$ as done, e.g., in (7) and (9) for some of the derivatives. Note also that $\mathbf{u}_1$ and $\dot{\mathbf{u}}_1$ are directly known because they are internal state of the controller.

We conclude the section enlightening a final property of the system in exam, that can result very useful in the planning phase, see, e.g., [14].

Corollary 2. *The system* (6) *is differentially flat and* $\mathbf{y}$ *is a flat output.*

Proof. The result is a direct consequence of the equivalence between dynamic feedback linearizability and differential flatness [15]. □

IV. NUMERICAL SIMULATIONS

We made the simulations in Simulink, and in particular we modeled the system using the toolbox *SimMechanics* in order to obtain a system model independent from the dynamic equations used for the control design.

The simulated system consists of two aerial vehicles of mass $m_{Ri} = 1\,[\mathrm{Kg}]$ and moment of inertia $J_{Ri} = 0.15\,[\mathrm{Kg\,m}^2]$, connected to the ground and to each other with two generic links of length $l_i = 2\,[\mathrm{m}]$, with $i = 1, 2$. The gains $\bar{\mathbf{K}}_1$ are chosen such as the error dynamic relative to φ_1 and φ_2 has poles in $(-3, -6, -9, -12)$. Similarly, the gains $\bar{\mathbf{K}}_2$ are chosen such as the error dynamic relative to f_{L1} and f_{L2} has poles in $(-4, -8)$. In order to verify the exponential

decreasing of the tracking error of the outputs, we set an initial error of $8°$ and $4°$ for φ_1 and φ_2 respectively, with respect the initial desired values. Similarly, for the stresses, we set an initial error of $5\,[\mathrm{N}]$ for f_{L1} and f_{L2}.

For the first simulation, whose results are shown in Fig. 3, the desired elevation trajectories are C^3 curves that generate a transition from the initial to the final configuration relative to the initial and final desired Cartesian position of the end of the chain, $\mathbf{p}_{B_2}(0) = [2\ 0\ 2]^T$ and $\mathbf{p}_{B_2}(T) = [-0.7\ 0\ 0.7]^T$, where 0 and T indicate the start and final time respectively. The values of the initial and final desired elevations are computed by standard inverse kinematics [16]. The desired stress is a C^1 trajectory that goes from the initial tension of $10\,[\mathrm{N}]$ to the final compression of $-10\,[\mathrm{N}]$, for both the links.

In the second simulation, whose results are shown in Fig. 4, the goal is to track an ellipsoidal trajectory of the end of the chain. For this purpose, given the desired trajectory of the second vehicle, by inverse kinematics, we computed the desired trajectories for the elevations. While the desired stress is a constant tension of $10\,[\mathrm{N}]$ for both the links.

Figs 3a and 4a show the desired and actual outputs, the inputs of the system, the tracking errors, the attitude of the vehicles and the desired an actual Cartesian coordinates. We can notice that, after a transient due to the initial errors, all the outputs converge to the desired trajectories. As expected we obtain zero tracking error also for stress trajectories that pass from tension to compression. In particular, in Fig. 3b, note how the thrust of first robot remains positive even when the tensions become negative, this happens because the compression is automatically obtained by turning the robot upside down. Figs 3b and 4b represent the evolution of the system along the trajectory through a sequence of images where the color define the time. The links are represented with a thinner dashed or a thicker solid line if the stress is a higher tension or a higher compression, respectively. Similarly, the thrust arrow is drawn thicker and longer when the thrust intensity is higher.

V. CONCLUSIONS

Considering a chained aerial system with two underactuated flying robots lying on a vertical plane, we designed a nonlinear controller able to steer the elevations and the stresses of the two links along any sufficiently smooth trajectory. This solution extends the previous literature in several directions, e.g., in a multi-agent sense thus allowing a much wider workspace. Moreover, exploiting the inverse kinematic of the system, we can track any smooth Cartesian trajectory of the second vehicle, while precisely and independently control the stresses on the links. Thus, the presented method could find, e.g., direct application on the aerial manipulation field, for tasks such as transportation and pick and place.

Future works will include: extension to a 3D scenario, to chain of n-links or to an arbitrary configuration of the connections between several robots.

REFERENCES

[1] R. Mahony and V. Kumar, "Aerial robotics and the quadrotor," *IEEE Robotics & Automation Magazine*, vol. 19, no. 3, p. 19, 2012.
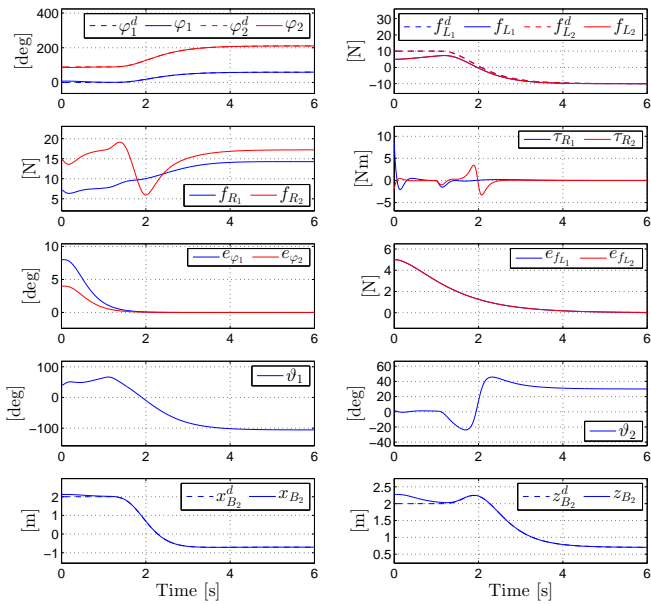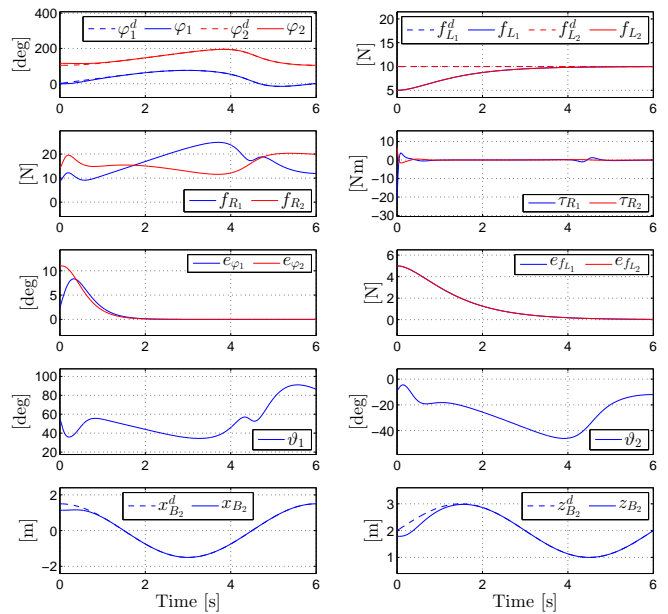
(a) Controller results: Notice that in the plots relative to the stress and its error the blue and red lines almost coincide.
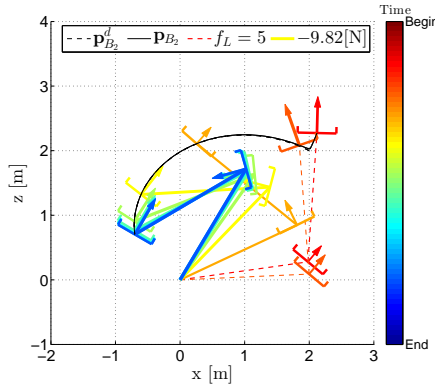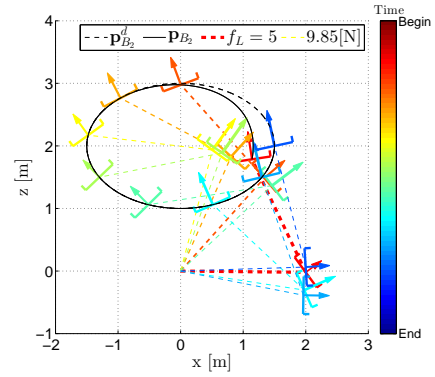

(b) Trajectory visualization from time Begin = 0 [s] to End = 6 [s].

Fig. 3: Class C^3 Cartesian trajectory of the end of the chain from the point $\mathbf{p}_{B_2}(0) = [2\ 0\ 2]^T$ to $\mathbf{p}_{B_2}(T) = [-0.7\ 0\ 0.7]^T$. The desired class C^1 trajectory for the stresses goes from the initial tension $f_{L_i}^d(0) = 10\,[\mathrm{N}]$ to the final compression $f_{L_i}^d(T) = -10\,[\mathrm{N}]$.

(a) Controller results: Notice that in the plots relative to the stress and its error the blue and red lines almost coincide.

(b) Trajectory visualization from time Begin = 0 [s] to End = 6 [s].

Fig. 4: Elipsoidal Cartesian trajectory of the end of the chain. The desired stress is a constant tension $f_{L_i}^d = 10\,[\mathrm{N}]$, with $i = 1, 2$.

[2] A. Franchi, C. Secchi, M. Ryll, H. H. Bülthoff, and P. Robuffo Giordano, "Shared control: Balancing autonomy and human assistance with a group of quadrotor UAVs," *IEEE Robotics & Automation Magazine, Special Issue on Aerial Robotics and the Quadrotor Platform*, vol. 19, no. 3, pp. 57–68, 2012.

[3] G. Gioioso, M. Ryll, D. Prattichizzo, H. H. Bülthoff, and A. Franchi, "Turning a near-hovering controlled quadrotor into a 3D force effector," in *2014 IEEE Int. Conf. on Robotics and Automation*, Hong Kong, China, May. 2014, pp. 6278–6284.

[4] I. Maza, K. Kondak, M. Bernard, and A. Ollero, "Multi-UAV cooperation and control for load transportation and deployment," *Journal of Intelligent & Robotics Systems*, vol. 57, no. 1-4, pp. 417–449, 2010.

[5] K. Sreenath and V. Kumar, "Dynamics, control and planning for cooperative manipulation of payloads suspended by cables from multiple quadrotor robots," in *Robotics: Science and Systems*, Berlin, Germany, June 2013.

[6] M. F. Pinkney, D. Hampel, and S. DiPierro, "Unmanned aerial vehicle (UAV) communications relay," in *Military Communications Conference, 1996*, vol. 1, Oct. 1996, pp. 47–51.

[7] F. Muttin, "Umbilical deployment modeling for tethered UAV detecting oil pollution from ship," *Applied Ocean Research*, vol. 33, no. 4, pp. 332–343, 2011.

[8] L. A. Sandino, M. Bejar, K. Kondak, and A. Ollero, "Advances in modeling and control of tethered unmanned helicopters to enhance hovering performance," *Journal of Intelligent & Robotics Systems*, vol. 73, no. 1-4, pp. 3–18, 2014.

[9] S. Lupashin and R. D'Andrea, "Stabilization of a flying vehicle on a taut tether using inertial sensing," in *2013 IEEE/RSJ Int. Conf. on Intelligent Robots and Systems*, Tokyo, Japan, Nov 2013, pp. 2432–2438.

[10] M. M. Nicotra, R. Naldi, and E. Garone, "Taut cable control of a tethered UAV," in *19th IFAC World Congress*, Cape Town, South Africa, Aug. 2014, pp. 3190–3195.

[11] M. Tognon and A. Franchi, "Nonlinear observer-based tracking control of link stress and elevation for a tethered aerial robot using inertial-only measurements," in *2015 IEEE Int. Conf. on Robotics and Automation*, Seattle, WA, May 2015.

[12] M. Cutler and J. P. How, "Actuator constrained trajectory generation and control for variable-pitch quadrotors," in *AIAA Guidance, Navigation, and Control Conference (GNC),(Minneapolis, Minnesota)*, 2012.

[13] H. K. Khalil, *Nonlinear Systems*, 3rd ed. Prentice Hall, 2001.

[14] H. Sira-Ramirez and S. K. Agrawal, *Differentially flat systems*. CRC Press, 2004.

[15] A. De Luca and G. Oriolo, "Trajectory planning and control for planar robots with passive last joint," *The International Journal of Robotics Research*, vol. 21, no. 5-6, pp. 575–590, 2002.

[16] B. Siciliano and O. Khatib, *Handbook of Robotics*. Springer, 2008.